Three-Dimensional Quantitative Co-Mapping of Pulmonary Morphology and Nanoparticle Distribution with Cellular Resolution in Nondissected Murine Lungs

Lin Yang,[†,‡,∥] Annette Feuchtinger,[§] Winfried Möller,[†,‡] Yaobo Ding,[†,‡] David Kutschke,[†,‡] Gabriele Möller,[#] Johannes C. Schittny,[¶] Gerald Burgstaller,[†,‡] Werner Hofmann,[□] Tobias Stoeger,[†,‡]Daniel Razansky,[⊥,∥], Alex Walch,[§] and Otmar Schmid[*,†,‡]

[†]Comprehensive Pneumology Center (CPC-M), Member of the German Center for Lung Research (DZL), Munich, 81377, Germany

[‡]Institute of Lung Biology and Disease, Helmholtz Zentrum München–German Research Center for Environmental Health, Neuherberg, 85764, Germany

[§]Research Unit Analytical Pathology, Helmholtz Zentrum München, Neuherberg, 85764, Germany

[⊥]Institute for Biological and Medical Imaging (IBMI), Helmholtz Zentrum München, Neuherberg, 85764, Germany

[∥]Faculty of Medicine, Technical University of Munich, Munich, 80333, Germany

[#]Department Genome Analysis Center, Institute of Experimental Genetics, Helmholtz Zentrum München, Neuherberg, 85764, Germany

[¶]Institute of Anatomy, University of Bern, CH-3012 Bern, Switzerland

[□]Department of Chemistry and Physics of Materials, University of Salzburg, Salzburg, A-5020, Austria

[*]**Corresponding author**

Dr. Otmar Schmid

E-mail: otmar.schmid@helmholtz-muenchen.de

Tel: +49-89-3187-2557. Fax: +49-89-3187-2400.

SI method 1: Calculation of absolute fluorophore intensity in NPs treated lungs

First, the total measured fluorescence intensity of a whole lung (including blank, instilled, and inhaled lungs) was determined by summing up all of fluorescence intensities of every single slice (automated segmentations of entire lung area defined by intensity thresholding using ImageJ). Principally, all the lungs should have the same (or at least very identical) level of tissue-induced autofluorescence under the same setting of light sheet fluorescence microscopy (LSFM) in the NPs-free regions. However, this is not true due to the measurement bias like variations in light penetration, tissue optical properties, and others. To reduce this error, correction for the total intensity of each lung should be performed based on tissue-induced autofluorescence. Briefly, we selected 4-5 representative NP-free regions of interest in the very edge of each slice (least light attenuation) at basically very similar position for each lung to achieve pixel auto-intensity in individual lung ($I_{i(p)}$) and then to calculate the average pixel auto-intensity from all lungs ($I_{av(p)}$). So for each lung, it has a specific correction factor $f = I_{av(p)}/I_{i(p)}$ and then its measured total fluorescence intensity should be corrected as Equation (1):

$$I_{c(t)} = I_{m(t)} * f \quad (1)$$

The terms $I_{c(t)}$ and $I_{m(t)}$ refer to the corrected and measured total fluorescence intensity, respectively.

For calculation of the tissue-induced autofluorenscence (I_{auto}) in NP treated lungs, it can be determined as in Equation (2):

$$I_{auto} = A * [\sum_{i=1}^{n} f(i) * \frac{I_{bl}}{A_{bl}}(i)]/n \quad (2)$$

A refers to total area of a NP treated lung. The term $\frac{I_{bl}}{A_{bl}}$ and *n* refer to the total area normalized-intensity obtained from the blank lungs and the used number of blank lungs, respectively.

The absolute intensity (I_{ab}) originated from fluorophore in NP treated lungs measured at channel for MF NPs (ex/em=640/30, 690/50) can be determined as seen in Equation (3):

$$I_{ab} = I_{c(t)} - I_{auto} \quad (3)$$

After correction, excellent linearity of fluorescence intensity-dose standard curve (R^2=0.994) was successfully achieved (Figure 5a).

SI method 2: Determination of tissue-induced autofluorecence in *C/P* and lobewise distribution analysis

C/P distribution analysis

Of note, the central and peripheral area of lung (lung slices) could have different levels of tissue-induced autofluorescence due to difference of lung structure (e.g. bigger lumen and higher intensity of airways in the center) indicating the autofluorescence in both regions should be separately determined. The Equation (2) can also be used to determine tissue-induced autofluorecence in center and periphery of NPs treated lungs. The only change is that both I_{bl} and A_{bl} should be obtained from the center (or periphery) regions (but not the total area used in SI method 1) in blank lungs, and then the autofluorecence intensity of center (or periphery) regions (A) of NP treated lungs can be determined separately. I_c (or I_p) used in the main text was calculated as the Equation 3.

Lobewise distribution analysis

In parallel with the C/P analysis, the lobewise specific autofluorescence should also be determined individually as different positioning and structure (e.g. amount of airways) of lobes in the lung might cause variations in the lobe-specific autofluorescence. This can be determined

by deformation of Equation (2), which lung area should be replaced by lung volume as different lobe has different volume.

$$I_{auto} = V * [\sum_{i=1}^{n} f(i) * \frac{I_{bl}}{A_{bl}}(i)]/n \quad (4)$$

V refers to total volume of a lobe from a NP treated lung. Again, both I_{bl} and A_{bl} should be obtained from the different lobes in blank lungs and then the lobewise autofluorecence intensity of NP treated lungs can be determined individually. Also, I_l (absolute NPs intensity in each lobe) used in the main text was calculated as the Equation 3.

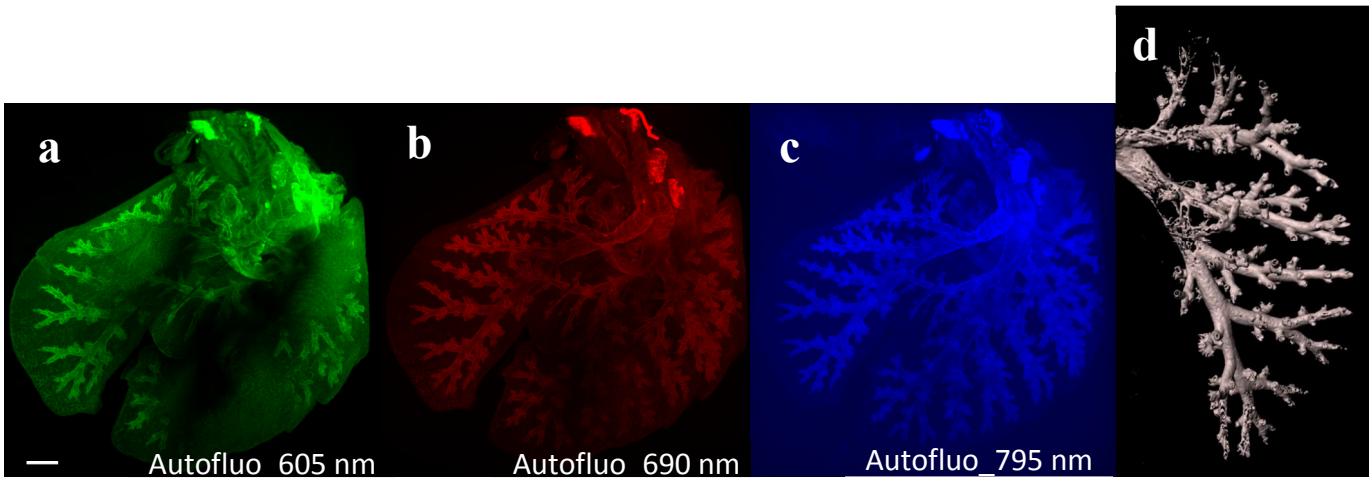

Figure S1 Visualization of lung morphology and airway structure generated from the tissue-induced autofluorencence of whole lung imaged using LSM at excitation and emission (ex/em) wavelengths of 545(30) / 605(70) (a), 640(30) / 690(50) (b), and 740(35) / 795(50) nm (c). 3D volume of lung image (maximum intensity projection) with better resolution can be achieved by using longer ex/em wavelength with higher penetration depth of laser light for occasionally poor perfused or cleared lungs. Clearly structure of the bronchial tree after surface rendering of left lobe of lung was easily identified (d). Scale bar 1000 µm.

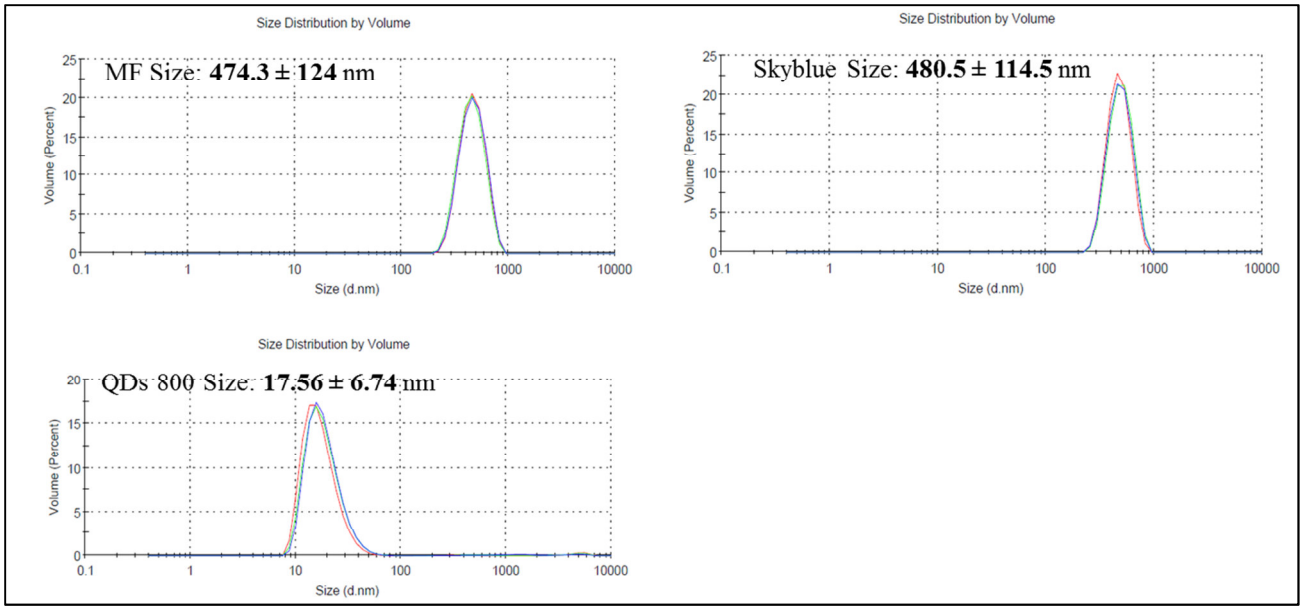

Figure S2: Volume-weighted size distribution of three types of nanoparticles suspended in distilled water that also used for pulmonary NP delivery measured using dynamic light scattering (DLS) in this study. All three NP suspensions were measured with a dilution factor of 1:50 from the respective stock suspensions. The size distribution of MF NPs was independent of the concentrations ranging from 25 mg/mL (stock suspension) to 0.125 mg/mL. Different colours of the curves indicate the three consecutive measurements for each sample and all of NPs exhibited uniform and stable size distribution.

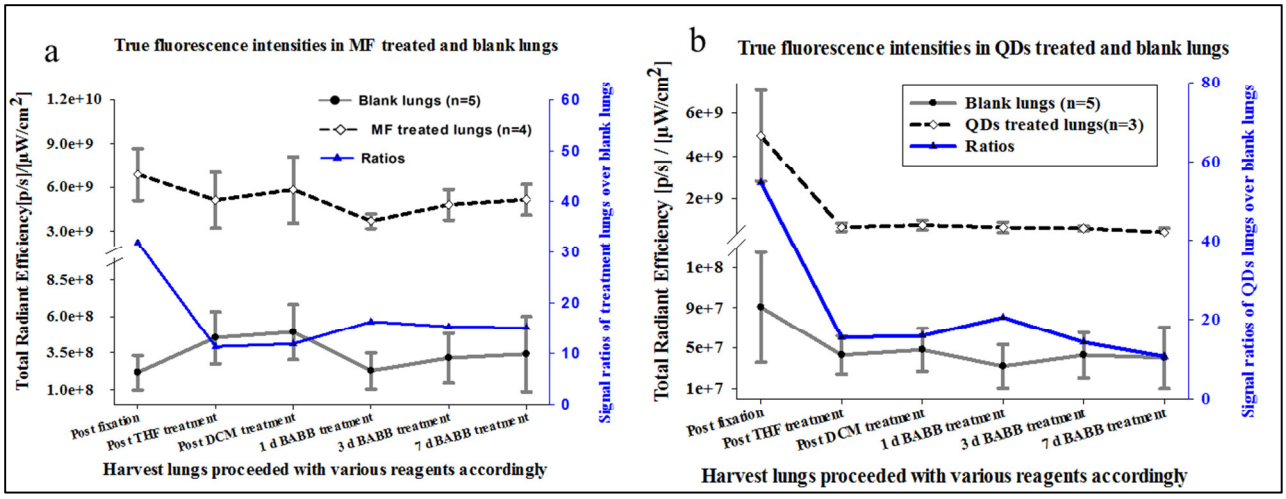

Figure S3: True fluorescence intensities in treated and blank lungs and the fluorescence ratio of treated lungs to blank lungs during tissue clearing. The lungs instilled with MF NPs (a) and QDs (b) at a dose of 62.5μg/lung and 40 pmol/lung, respectively were measured by using In Vivo Imaging System (IVIS). The fluorescence signals of lungs contained NPs were not statistically changed during tissue clearing especially for MF NPs, representing both of NPs fluorescence can be well preserved. Also, the ratio of fluorescence signal in treated lungs to blank lungs is of 10-20 indicates these NP fluorescence can be easily detected by later light sheet fluorescence microscopy.

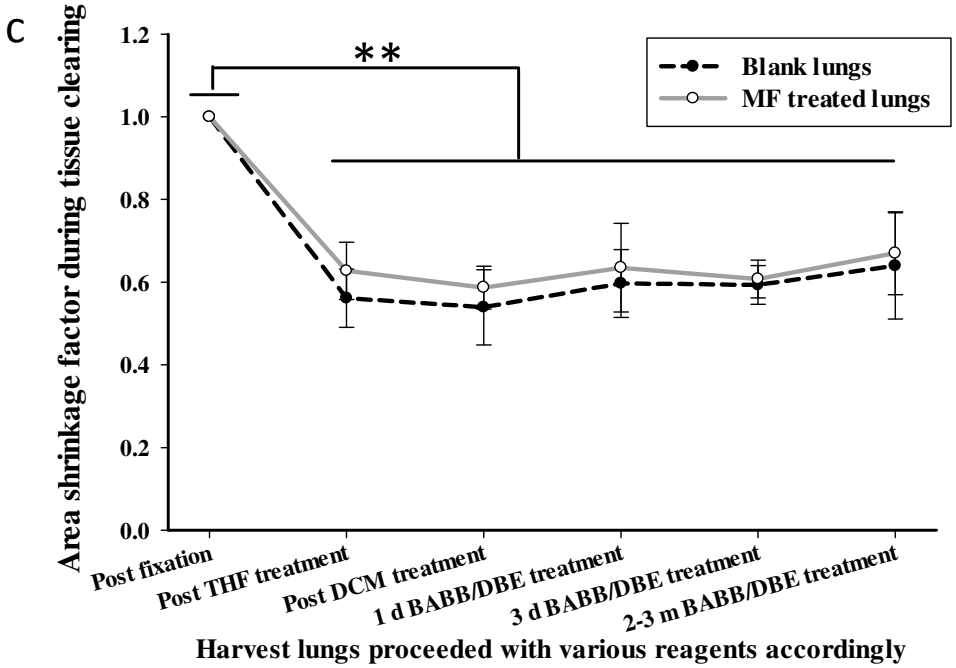

Figure S4: Area shrinkage factor during tissue clearance for blank and MF treated lungs. This data was achieved from the IVIS measurement of lung geometric area. The projected area in each step was normalized to the first step (post fixation). Around 37-44% shrinkage of lung projected area after THF treatment but no further change after 1 day DBE treatment. And as expected, no significant difference in lung shrinkage between blank lungs and treated lungs was found.

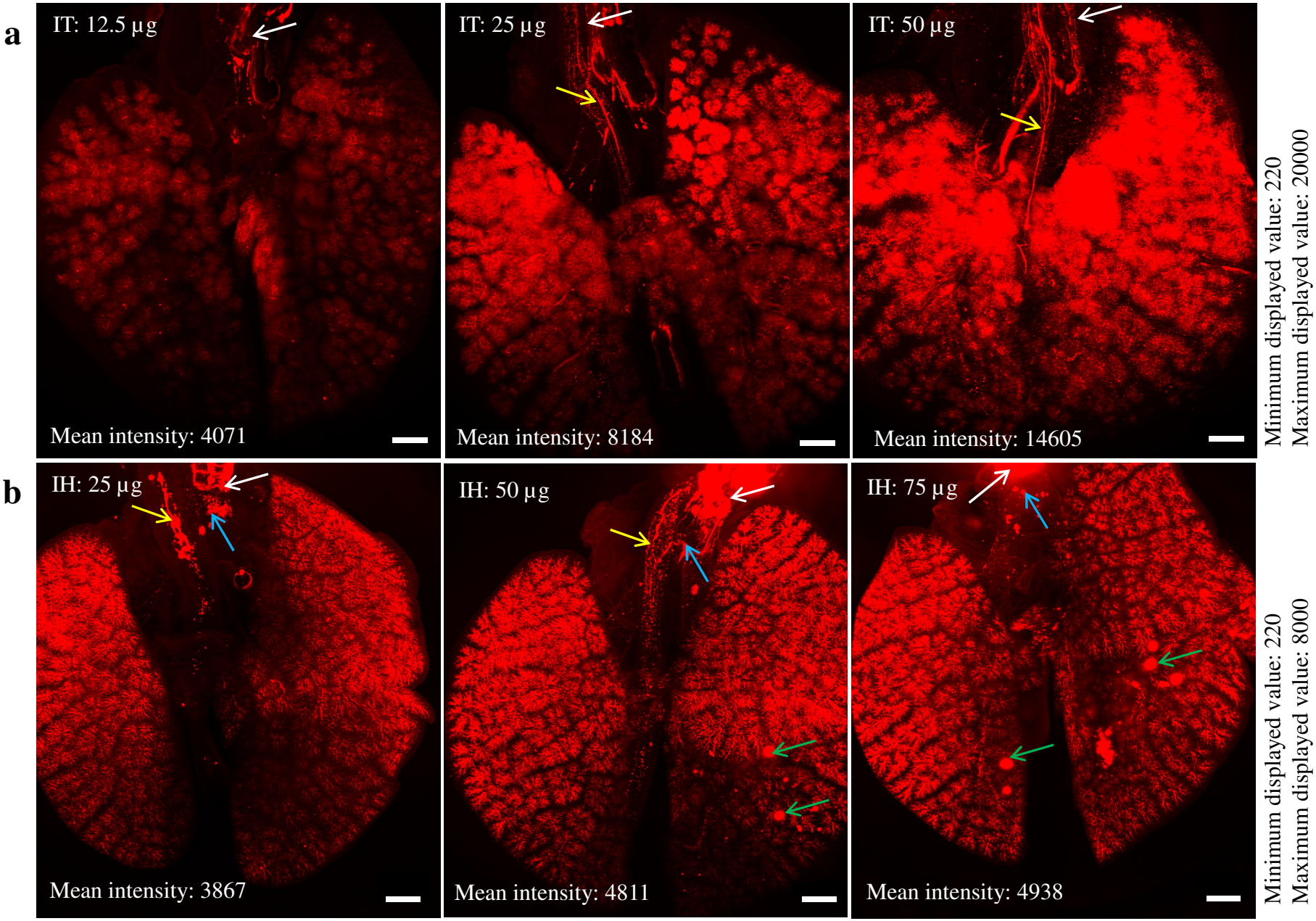

Figure S5: 3D visualization of melamine resin NP distribution pattern in whole lung after intratracheal instillation and inhalation

exposures. a: three instilled lung images (generated from ImageJ with maximum intensity projection, MIP) with three applied doses (12.5 µg, 25 µg, and 50 µg) shows the gradually increased mean fluorescence intensity of NPs. This indicates that strong linear relationship of the fluorescence intensity-instilled dose which can be reliably used to determine the inhaled dose for inhalation exposure. b: three inhaled lungs images (MIP) with three applied doses (25 µg, 50 µg, and 75 µg) did not show significantly enhanced fluorescence intensity which refers to inhalation could lead to bigger variations in deposited doses of lung than instillation. As seem from (a) and (b), 3D distribution of NP varied significantly for different application routes. Inhalation exhibited a homogeneous distribution whereas preferentially proximal airway and acinar deposition in instillation. White arrows indicate the NP deposited to the trachea regions in both application routes but seems higher deposition ratios in inhalation exposure, yellow arrows mark the NPs can be transferred to the esophagus immediately after both exposures, and green arrows designate some droplet could be formed, transported, and stuck in lower airways during aerosol inhalation. Scale bar: 1000 µm.

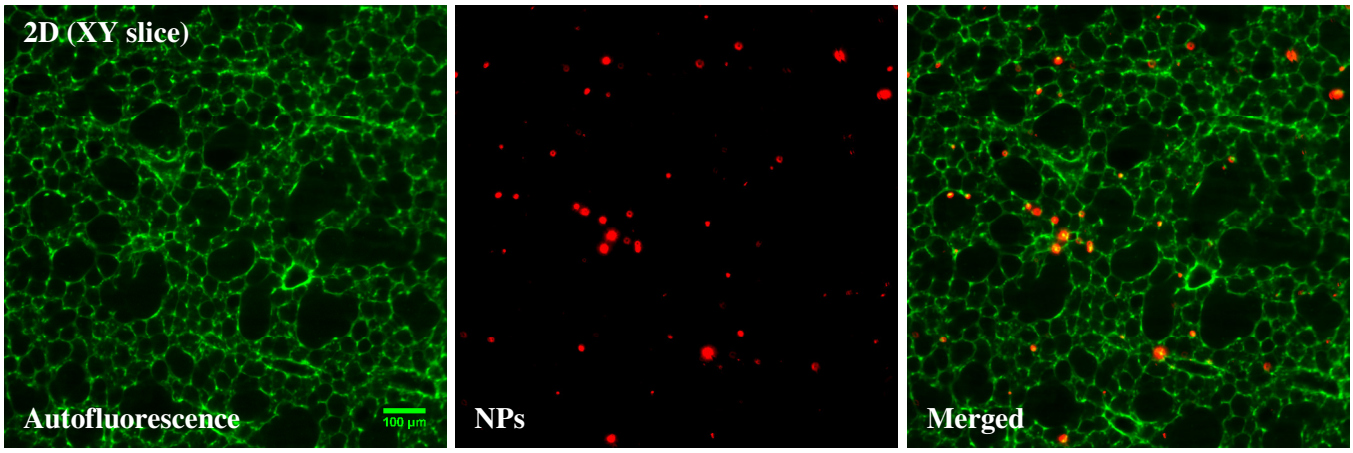

Figure S6: Visualization of MF NPs distribution (red) at single-cell resolution in a 2D image of an inflated murine lung at 24 h after inhalation. Similar to intratracheal instillation (Figure 4C and 4D) micron-sized NP agglomerates were found 24 h after inhalation which is likely due to phagocytic NP uptake by macrophages.

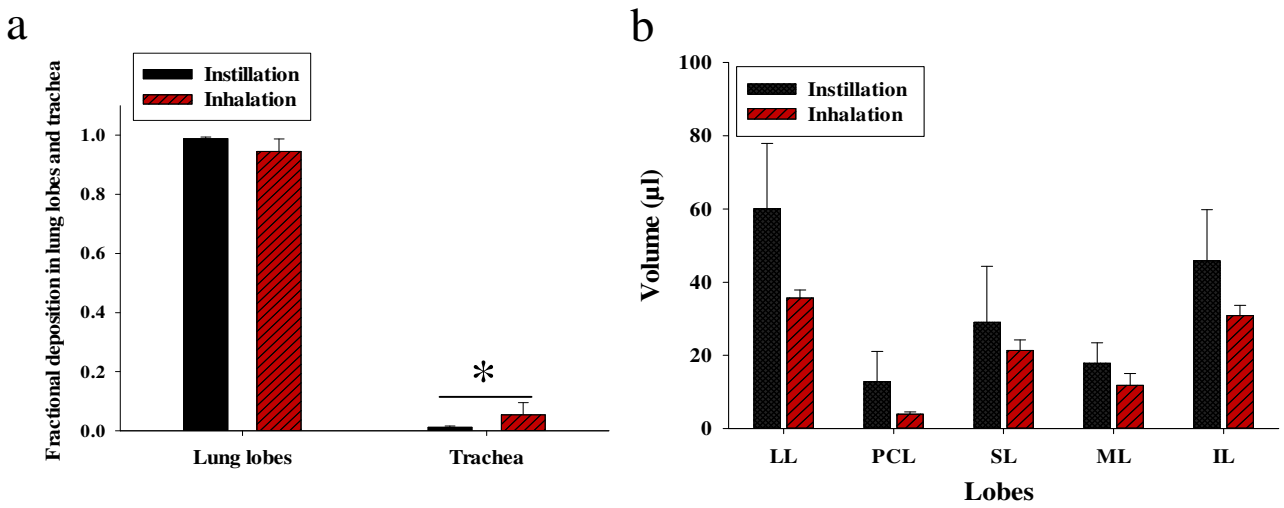

Figure S7: Quantitative analysis of fractional deposition of MF NPs in lung lobes and trachea (a) and lobe volume (b) for both application routes. As displayed in a, most of NPs deposited in lung lobes compared to the respiratory tract (here: only trachea). But inhalation showed significantly higher ratio of trachea to total pulmonary deposition than that in instillation. Of note, the trachea regions was not totally imaged due to the size limitation of the LSFM, which might contributing to the low amount of deposition. The lung volume was directly measured from LSFM images without shrinkage corrections. Abbreviations of lung lobes, LL: left lung; PCL: postcaval lobe; SL: superior lobe; ML: middle lobe; IL: inferior lobe.

Video legends

Video S1

3D reconstruction of a whole lung architecture scanned by light sheet fluorescence microscopy. The 3DISCO clearing protocol renders the whole murine lung fully transparent, allowing for visualization of the entire bronchial tree (green) along the trachea, over primary bronchus to the small bronchioles in autofluorescent channel (ex/em=545/605 nm).

Video S2

3D mapping of the MF NP distribution pattern in a murine lung after intratracheal instillation obtained by LSFM. The NPs are shown in red and tissue structure in green. MF was found deposited along the bronchial tree starting from trachea down to the terminal bronchioles and into the alveoli. The patchy and preferentially central and upper airway and acinar deposition pattern for instillation is evident.

Video S3

3D mapping of the MF NP distribution pattern in a murine lung after intratracheal aerosol inhalation obtained by LSFM. The NPs are shown in red and tissue structure in green. Inhalation of aerosolized NPs displays a uniform pulmonary NP distribution pattern in the proximal and distal airways and acini, which it is much more even than instillation of NPs.

Video S4

Cellular-resolution visualization of NP localization in alveolar regions of an agar-filled inflated lung of a mouse at 24 h after NP instillation imaged using LSFM. The NPs are shown in red/yellow and tissue structure in green. The details of NPs deposited in fine alveolar structure are clearly visible in 2D orthoslicing and the large NP agglomerates accumulated in the individual alveolar sacs was potentially due to the macrophage uptake.

Video S5

Cellular-resolution visualization of NP localization in alveolar sacs of an agar-filled inflated lung of a mouse at 24 h after NP instillation scanned using confocal microscopy. The NPs are shown in red/yellow and tissue structure in green. The NPs located in alveolar septum is clearly seen in both 3D reconstruction and 2D orthoslicing.

Video S6

3D visualization of MF transportation and accumulation (red) in the esophagus of a mouse (gray) immediately (<3 min) after administration. This clearly exhibits that NPs can be cleared within a few minutes toward the digestive tract by either mucociliary clearance or coughing.